



Street network patterns for mitigating urban heat islands in arid climates

Kimia Chenary, Ali Soltani & Ayyoob Sharifi

To cite this article: Kimia Chenary, Ali Soltani & Ayyoob Sharifi (2023) Street network patterns for mitigating urban heat islands in arid climates, International Journal of Digital Earth, 16:1, 3145-3161, DOI: [10.1080/17538947.2023.2243901](https://doi.org/10.1080/17538947.2023.2243901)

To link to this article: <https://doi.org/10.1080/17538947.2023.2243901>



© 2023 The Author(s). Published by Informa UK Limited, trading as Taylor & Francis Group



Published online: 10 Aug 2023.



Submit your article to this journal [↗](#)



Article views: 2240



View related articles [↗](#)



View Crossmark data [↗](#)



Citing articles: 11 View citing articles [↗](#)



Street network patterns for mitigating urban heat islands in arid climates

Kimia Chenary^a, Ali Soltani ^{b,c,d} and Ayyoob Sharifi ^e

^aDepartment of Architecture and Urban Planning, Bojnourd University, Bojnourd, Iran; ^bInjury Studies, FHMRI, Bedford Park, Australia; ^cUniSA Business, University of South Australia, Adelaide, Australia; ^dDepartment of Urban Planning, Shiraz University, Shiraz, Iran; ^eThe IDEC Institute and Network for Education and Research on Peace and Sustainability (NERPS), Hiroshima University, Higashihiroshima, Japan

ABSTRACT

This study explores the impact of street pattern measurements on urban heat islands (UHI) in the arid climate of Mashhad, Iran. The Landsat-8 top-of-the-atmosphere (TOA) brightness images from 2013 to 2021, average values of normalized difference vegetation index (NDVI) and land surface temperature (LST) were calculated. Street pattern measurements, including closeness-centrality, straightness, and street orientation, were employed to analyse the patterns in each district. The results indicated that districts with higher straightness and lower closeness-centrality exhibit cooler surface temperatures. Strong correlations were observed between LST and NDVI, straightness, and local closeness-centrality. The research highlighted the importance of considering street network measurements in long-term urban planning and design to mitigate the UHI effect in arid regions. A moderate grid street pattern with a reasonable distribution of green spaces throughout the region is suggested to reduce surface temperatures sustainably. Street pattern indexes, such as straightness and local closeness-centrality, are identified as significant factors in urban design to mitigate UHI. These findings have implications for urban planners, who can use this information to create street network patterns with lower UHI effects by reducing local closeness-centrality and increasing straightness.

ARTICLE HISTORY

Received 25 April 2023

Accepted 27 July 2023

KEYWORDS



Urban heat island; Urban form; Street network pattern; Green space distribution

Highlights

- Importance of street network measurements in mitigating UHI in arid regions.
- Moderate grid pattern with green spaces reduces surface temperatures sustainably.
- Incorporating street pattern indexes and NDVI distribution for urban resilience and heat reduction.

1. Introduction

Since 200 years ago, urban heat islands (UHI) have been widely discussed as a difference in the temperature between the built environment and the surrounding natural environment (Howard

CONTACT Ali Soltani  ali.soltani@flinders.edu.au  Injury Studies, FHMRI, Bedford Park, South Australia 5042, Australia

© 2023 The Author(s). Published by Informa UK Limited, trading as Taylor & Francis Group

This is an Open Access article distributed under the terms of the Creative Commons Attribution License (<http://creativecommons.org/licenses/by/4.0/>), which permits unrestricted use, distribution, and reproduction in any medium, provided the original work is properly cited. The terms on which this article has been published allow the posting of the Accepted Manuscript in a repository by the author(s) or with their consent.

1818). Increasing temperatures are a global concern, as people live with devastating extreme weather exacerbated by rising temperatures. The increasing temperature level has resulted in severe weather conditions and the extinction of several species (Solomon et al. 2007).

Iran's surface average temperature has risen by around 0.85°C during the last 60 years, which is higher than the global average temperature (Amanzadeh et al. 2021). Furthermore, Iran is located in an arid region. With an average annual water consumption of 8% more than the total renewable water resources and about 80% more than the country's scarcity threshold (Mesgaran and Azadi 2018; Qasemipour et al. 2020). Moreover, Iran's energy consumption exceeds the global average by 4.4 times, and it is among the top ten countries releasing greenhouse gases during the next few years (Sadeqi, Tabari, and Dinpashoh 2022). Given the importance of cooling cities for reducing energy consumption, it is crucial to mitigate UHI.

UHI impact Iranian metropolises such as Tehran, Mashhad, Tabriz, Shiraz and Ahwaz for numerous causes (Bagheri and Soltani 2023). Due to the lack of vegetation and increased surface coverage by buildings, roads, and concrete, sprawling cities and low-density metropolitan areas with insufficient green space contribute to urban heat islands (UHI). The absence of foliage and altered wind patterns exacerbate heat retention and release, resulting in higher daytime temperatures and warmer nighttime temperatures. In addition, diminished thermal regulation and increased energy consumption from air conditioning intensify UHI effects. In addition, urban decay and the transfer of urban centres and central business districts (CBDs) to outer rings (Moghadam et al. 2018b; Moghadam, Soltani, and Parolin 2018a) can worsen UHI effects by abandoning heat-absorbing infrastructure and increasing heat emissions from expanded transportation networks to these outer areas.

Wind and clouds affect UHI and solar energy transit. Most Iranian metropolises are inland and surrounded by high mountains, hindering natural circulation (Voogt 2004). Most are on low ground with strong winds. Rural areas that are cooler at night have been absorbed by low-density urban development (Azhdari, Soltani, and Alidadi 2018). Roadways and housing complexes have created the greatest heat island impact. High-rise buildings, especially in outer suburbs and urban fringes, have affected wind speeds and assisted in creation of UHI. Replacing natural surfaces with impermeable surfaces like highways, parking lots, and buildings has made urban areas drier and less water available for evaporation (E. Sharifi and Soltani 2017). The excessive also energy usage per capita, mostly from interior heating and cooling and transportation, has raised near-surface air temperatures. Air pollution in Iranian metropolises, Ahwaz, and other cities absorbs radiation in the lower troposphere, forming an inversion layer that prevents rising air from fleeing the region (Rosenzweig, Gaffin, and Parshall 2006). Land use and urban planning also contribute to the UHI effect in Iranian metropolises. Urban regions have greater surface temperatures than rural places because concrete and asphalt surfaces absorb and retain solar radiation and lack natural spaces and trees. Urban form and building design affect shading, ventilation, and heat absorption. Narrow streets and streets without appropriate ventilation may trap heat, creating UHI. Inefficient physical development and transportation energy consumption and fossil fuel use generate GHG and other pollutants that trap heat in the lower atmosphere, aggravating the UHI effect.

Surface temperatures are affected by various urban parameters (E. Kong et al. 2021; Sharifi and Soltani 2017). Among other things, these include land cover, building materials, population density, and vegetation cover (Abdollahzadeh and Boloria 2021; Wu et al. 2018). Furthermore, urban form parameters such as urban blocks, building heights, street widths, street orientations, urban street networks measurements, and building volumes are important (Kim and Brown 2021). Moreover, there is a spatial difference in land surface temperature (LST) and urban morphology indicators, such as building density, building height, floor area ratio, sky view factor, and frontal area index (Han et al. 2022). Research has shown that diurnal and nocturnal UHI intensity (UHII) have different patterns across different gradients, which can be used to guide urban planning decisions (Yang et al. 2022). In order to identify new UHI patches produced through infilling, edge expansion, and leapfrogging, an index of UHI expansion (UHIEI) has been developed (Qiao et al. 2023).

Based on simulations of building and green space arrangements, the local climate zones that affect urban thermal comfort are investigated (Ren et al. 2022). It was found that UHI can be reduced by using green roofs and walls or by adjusting the colour of buildings (Kim and Brown 2021; Kong et al. 2021). While several studies have been conducted to optimize green roofs, these methods are inapplicable on a metropolitan scale and arid climate (Tan and Wang 2023; Tan, Qin, and Wang 2022). Moreover, the arid climate makes the use of light colours that reduce heating inside the building unsustainable (Lee et al. 2020; Naserikia et al. 2019). Therefore, in order to mitigate UHI in arid climate, one strategy could be working on urban street patterns and normalized difference vegetation index (NDVI) distribution in different neighbourhood should be considered. Organic curvilinear street pattern represents angular routes, oriented in various directions. Grid street pattern is a feature of planned development or newly founded settlements. Grid forms often give rise to bilateral directionality on a broader scale. Grid and semi-grid patterns provide equal land division and greater control over growth. Modern hierarchical layouts curvilinear are often associated with curvilinear loops of distributor roads, forming looping or branching patterns (Marshall 2004; Masoumi 2015).

Some studies found that green spaces between building blocks, such as street trees and neighbourhood pocket parks, can reduce UHI (Hou et al. 2022; Kleerekoper, Van Esch, and Salcedo 2018; Song et al. 2020). It was found that different street layouts have different impacts on UHI (Abdollahzadeh and Biloría 2021; Erdem, Mert Cubukcu, and Sharifi 2021; Mohamed et al. 2021; Sobstyl et al. 2017). In fact, the morphology of urban streets can help improving urban microclimate, through reducing energy, and lowering GHG emissions. The street network features such as centrality, connectivity, street width, edge, and orientation are correlated with UHI (A. Sharifi 2019). The network connectivity, and network centrality are associated with the level of UHI (Erdem, Mert Cubukcu, and Sharifi 2021). The local closeness-centrality, betweenness, and straightness were found as appropriate metrics to analyse the street network structure (Porta, Crucitti, and Latora 2006). Street morphology was found to be correlated to LST in the metropolitan Tehran (Ghanbari et al. 2023).

The research contribution of this paper is to provide insight into the importance of considering street network measurements in long-term urban planning and design to mitigate the UHI effect in arid regions. The study suggests that a moderate grid street pattern with a reasonable distribution of green spaces throughout the region can help reduce surface temperatures sustainably. It also highlights the significance of street pattern indexes, such as straightness and local closeness-centrality, in urban design to mitigate the UHI effect.

2. Study area

Mashhad is the Iran's second metropolitan area with a population of more than 3 million. It is located in Razavi Khorasan province occupying an area of about 370 square kilometres. Mashhad is located between the two mountain ranges of Binalood and Hezar-masjed, in the valley of the Kashaf River near Turkmenistan (Figure 1). Mashhad has a special continental climate due to the interaction of different air masses. Polar continental, maritime tropical, and Sudanese air masses affect this location (Zendehbad et al. 2019). Generally, it has a dry and cold climate, with summers that are hot and dry, and winters that are wet and cold (Nasseh et al. 2016). There is an average annual rainfall of 253 millimetres, with most of the precipitation falling between February and March. Mashhad, as many metropolises in West Asia, has seen a considerable change in its land cover/land use, particularly from green areas to residential and industrial, which has led to an increase in the amount of heat and emissions generated in the city (Allan et al. 2022; Azizi et al. 2022).

In Mashhad, the historical area is situated in the east and is composed of old fabric limited to modern movements and lack sufficient open spaces (Masoumi 2015). Over time, Mashhad expanded from east to west. The city of Mashhad consists of 12 districts. There is a holy shrine

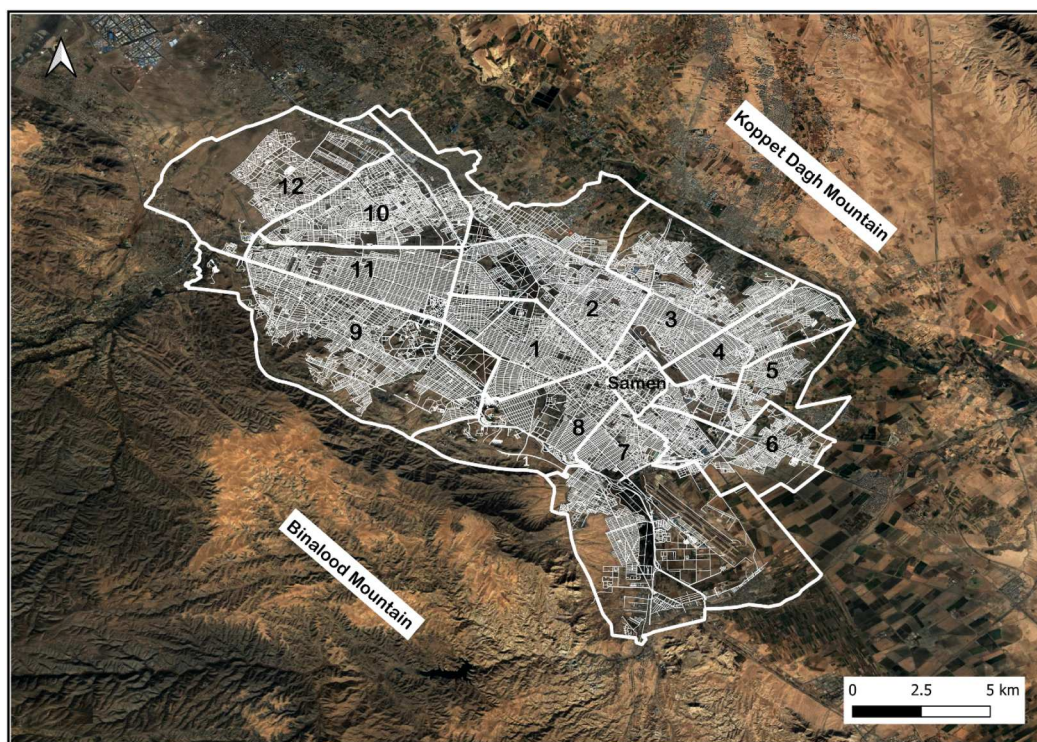


Figure 1. Mashhad metropolitan area.

in Samen district which is one of the most important pilgrimage areas. There are four districts in the mid-eastern region of the city that provide pilgrimage services: 1, 3, 4, 5, 6 and 8. The mid-western zone, which includes districts 1, 2 and 9, is separate from pilgrimage. The north-western zone, which consists of district 10 and district 12, is a new residential development. Districts 11 and 9 are located in the south-west zone, which is a new residential zone with amenities and recreational facilities (Ramyar 2019). The districts of Mashhad can be classified basing on their physical characteristics and capabilities. As a result of this classification, we were able to limit our study to four different districts. Table 1 provides the detailed information on: area, density, street network area of each district (Table 1).

3. Materials and methods

A mixed of remote sensing tools including Google Earth Engine (GEE), network analysis, and image processing was used (Table 2). To begin, we visualized the average NDVI and LST for the period 2013–2021 using GEE. However, when comparing these two indexes, it became evident that a higher NDVI degree is not necessarily associated with a lower surface temperature. As satellite imagery includes heat from all aspects of a city, in addition to the NDVI, other urban indexes can also impact LST (Portela et al. 2020). Considering that the NDVI degree alone is not an effective means of UHI, we begin to analyse other urban factors on LST, such as street patterns and breathing spaces between buildings. We analyse the street network patterns using the Python OSMnx and Momepy libraries to analyse their impact on LST; The OpenCV Python library made it possible to examine the distribution of green spaces between building blocks (Table 3).

Table 1. Details of 13 urban districts of Mashhad.

Name of districts	Area (hectare)	Population (thousand)	Population Density (people/hectare)	Street network area (hectare)
Districts 1	1474	168,135	114	474
Districts 2	3825	510,338	133	2004
Districts 3	3308	382,821	115	2110
Districts 4	1345	261,598	194	648
Districts 5	1439	174,076	120	823
Districts 6	1924	232,526	120	1109
Districts 7	5661	261,071	46	2449
Districts 8	1982	88,916	45	933
Districts 9	4567	343,950	75	2471
Districts 10	2290	296,110	117	1051
Districts 11	1579	199,706	126	739
Districts 12	6763	86,039	12	5699
Samen district	350	13,849	39	104

3.1. Estimation of land surface temperature (LST)

The GEE catalogue contains images of Landsat-8 top-of-the-atmosphere (TOA) brightness, which eliminates the need to calculate top of the atmosphere spectral radiance and brightness temperature. We calculated the mean of LST from 01/01/2013 to 31/12/2021 for the case study area.

There are two instruments on the Landsat 8 satellite payload: the Operational Land Imager (OLI) and the Thermal Infrared Sensor (TIRS). With a spatial resolution of 30 metres (visible, NIR, SWIR); 100 metres (thermal); and 15 metres (panchromatic), these sensors provide seasonal coverage of the global landmass (Irons, Dwyer, and Barsi 2012). We visualized LST using the TOA image collection's thermal bands (band 10) with a spatial resolution of 100 m. Table 4 shows the list of Landsat-8 OLI and TIRS bands.

3.2. Estimation of normalized difference vegetation index (NDVI)

Landsat near-infrared and visible bands were used to calculate NDVI. The result of the NDVI formula generates a value between -1 and $+1$ (Alves, Anjos, and Galvani 2020). Healthy vegetation reflects more near-infrared (NIR), but it absorbs more red and blue light. Healthy vegetation has a low value in the red channel and a high value in the NIR channel, which yields a high NDVI value (Yang et al. 2019).

$$\text{NDVI} = \frac{\text{NIR (Band 5)} - \text{Red (Band 4)}}{\text{NIR (Band 5)} + \text{Red (Band 4)}} \quad (1)$$

where NIR is represents the near-infrared band (Band 5) and red is represents the red band (Band 4) (Nagy et al. 2021).

3.3. Estimation of NDVI distribution

We conducted this analysis in order to estimate the distribution of vegetated areas using grey NDVI images. The pixels of the images were calculated according to grey brightness with OpenCV. Following that, the values were counted and visualized as a histogram. OpenCV is a huge open-source

Table 2. Data and methods.

Data source	Method	Open-source tools	Indices
Landsat-8 Data Collection of GEE	Imagery analysis	GEE	LST, NDVI
Open Street Map	Network analysis	Python	Straightness, Local closeness-centrality
NDVI in Greyscale	Image processing	Python	NDVI distribution

Table 3. Details the measures applied in this research.

Measurements			Application		How it works	References
Street Network	Street Straightness		Straight connectivity between two nodes			
	Street Edge Bearing		The compass bearing from each directed edge's origin node U to its destination V		Grid pattern with longer and straighter streets representing higher straightness, while loops and trees represent lower straightness.	Altaweel, Hanson, and Squitieri (2021), Erdem, Mert Cubukcu, and Sharifi (2021), Sharifi (2019)
	Street Local-Closeness Centrality		The shortest distance between nodes to every other node		More scattering of street edge bearing represents loop and dendritic street patterns, while the low scattering of street angles represents grid pattern.	Boeing (2017), Barthelemy (2022)
Green Spaces	NDVI Distribution		The greyscale image pixel intensity values		The high level of local closeness-centrality represents the loop and tree pattern, while the low level represents the grid pattern.	Erdem, Mert Cubukcu, and Sharifi 2021; Sharifi (2019)
	Normalized Difference Vegetation Index(NDVI)		The difference between vegetation and bare soil		As dark areas in a greyscale image are defined as vegetated lands, more pixels with dark values represent a greater distribution of vegetated lands.	Abd Elaziz et al. (2021)
					Typically, built-up and bare soil areas indicated low NDVI degrees, while the vegetated area indicated moderate.	Yang et al. (2019), Alves, Anjos, and Galvani (2020)

Table 4. Landsat-8 OLI and TIRS bands performance requirements.

	Bands	Wave length (micrometres)	Resolution (metres)
Landsat-8 OLI and TIRS bands	Band 1 – Coastal aerosol	0.43 - 0.45	30
	Band 2 – Blue	0.45 - 0.51	30
	Band 3 – Green	0.53 - 0.59	30
	Band 4 – Red	0.64 - 0.67	30
	Band 5 – Near Infrared (NIR)	0.85 - 0.88	30
	Band 6 – SWIR 1	1.57 - 1.65	30
	Band 7 – SWIR 2	2.11 - 2.29	30
	Band 8 – Panchromatic	0.50 - 0.68	15
	Band 9 – Cirrus	1.36 - 1.38	30
	Band 10 – Thermal Infrared	10.60 - 11.19	100
	Band 11 – Thermal Infrared	11.50 - 12.51	100

library for image processing that calculates the specific image's pixel value based on grey brightness and gives the output of arrays from the image (Abd Elaziz et al. 2021).

3.4. Network analysis

In case, the NDVI degree alone could not explain the UHI, we looked for other urban factors that could have affected the UHI. This section discusses the impact of the urban street network on LST by classifying different types of patterns (Omer and Zafrir-Reuven 2015). Momepy and OSMnx open-source tools were used: local closeness-centrality, and straightness. The morphology of street network can be analysed using Graph theory focusing on vertex, node, links or edges between them (Boeing 2017). A street network is considered a sample of a complex spatial network, including nodes and edges embedded in space (Barthelemy 2022).

3.4.1. Estimation of street local closeness-centrality

The purpose of calculating the inverse of the short path length average is to discover the shortest distance between nodes in a network, considering different types of networks (Grubb et al. 2021; Lin and Ban 2017). Grid patterns are longer than loop patterns, therefore elements in loop patterns are closer to each other than in grid patterns. We visualized local closeness-centrality using a Python library called Momepy provides tools for network morphometric analysis. These tools are capable of describing urban forms in a reproducible and scalable manner as part of modern data science frameworks (Fleischmann, Feliciotti, and Kerr 2022).

$$C(u) = \frac{n - 1}{\sum_{v=1}^{n-1} d(v, u)} \quad (2)$$

where n is the number of nodes and $d(v, u)$ is the shortest path length between v and u (Lin and Ban 2017).

3.4.2. Estimation of street straightness

Straightness indexes categorize different network structures based on straight lines. This index measures the straight connectivity between two nodes. There is a greater degree of straightness in the grid network as compared to the loop network (Altaweel, Hanson, and Squitieri 2021).

$$C_s(i) = \frac{1}{n - 1} \sum_{j \in v, j \neq i} \frac{d_{ij}^{Eu}}{d_{ij}} \quad (3)$$

where n = the number of nodes; d_{ij}^{Eu} = the Euclidean distance between nodes i and j along a straight line and d_{ij} = the shortest path length between i and j .

4. Result

We present the results in three sections: Visualization which includes NDVI and LST visualization. We provided this section for the calculation of LST and NDVI values. The purpose of this section was to analyse the impact of NDVI degrees on LST. An analysis of network measurements was conducted to compare and understand the effects of network measurements on LST, including local closeness-centrality, and straightness. An image processing technique was used in the analysis of NDVI distribution in order to determine the effects of green space distribution on LST.

4.1. LST variation in all districts of the study area

Hundred cloud-free images were used to create LST with the resolution of 100 m from winter 2013 to winter 2021. Figure 2 shows that the same LST value was used for all districts in Mashhad city, Iran, ranging from 10 [?] to 26[?]. Median surface temperatures were recorded for each district, with district 1 having the lowest temperature at 20.35[?]. District 9 had a slightly higher temperature of 21.93[?] compared to district 8 at 21.81[?], while district 11 had a temperature of 22.07°C. Samen district, district 6, and district 7 had temperatures of 22.22°C, 22.54°C, and 22.84°C, respectively. District 2, district 10, and district 3 had temperatures of 23.02°C, 23.16°C, and 23.30°C, respectively, while district 5 had the highest temperature at 23.39°C, followed by district 4 at 24.30°C. The lowest temperature is recorded in district 1, at 20.35[?]. The temperature in district 9 is 21.93[?], which is slightly higher than that in district 8, which is 21.81[?]. The temperature in district 11 was 22.07°C. Temperature values were 22.22°C, 22.54°C, and 22.84°C in Samen district, district 6, and district 7 respectively. Temperature values in district 2, district 10, and district 3 was 23.02°C, 23.16°C, and 23.30°C, respectively. District 5 has the highest temperature at 23.39°C, followed by district 4 at 24.30. The boxplots indicate that each district had almost the same temperature range.

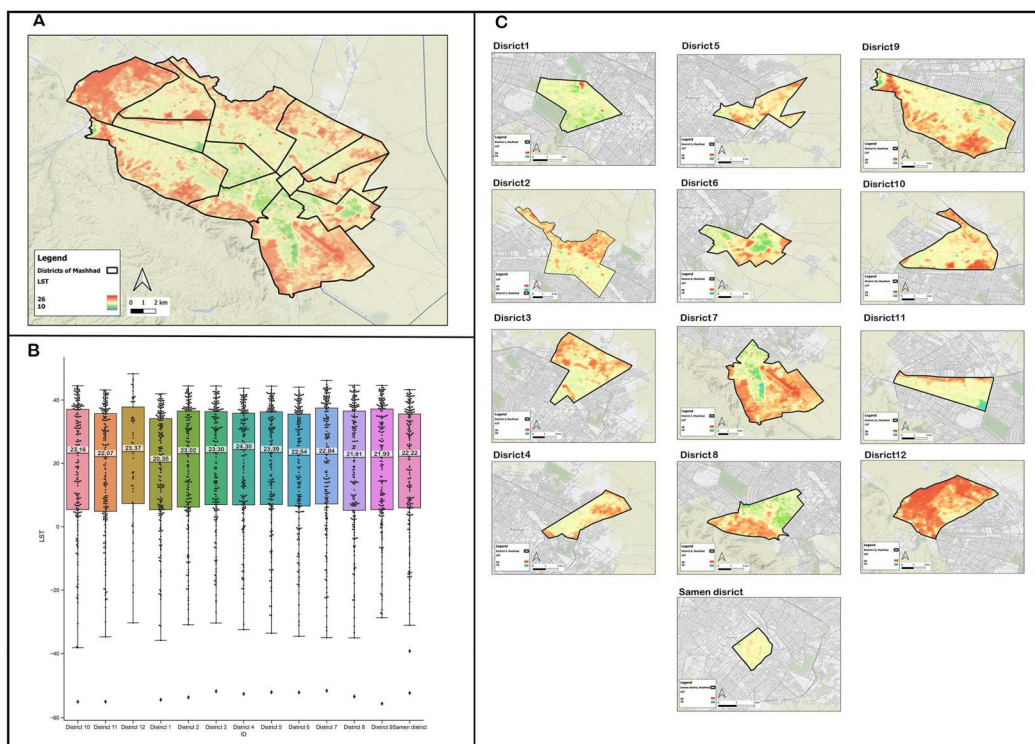


Figure 2. (A) LST variation; (B) Comparison median LST of all districts; (C) Comparison LST of all districts.

4.2. NDVI variation in all districts of the study area

Hundred cloud-free images were used to create the NDVI map with the resolution of 30 from winter 2013 to winter 2021, using GEE image collection of Landsat-8 top-of-the-atmosphere (TOA) brightness. As can be seen in Figure 3 shows all NDVI values ranged from -0.5 to 0.7 . The highest value is assigned to district 12 (0.042). This was followed by district 7, at 0.041 . NDVI value of district 3 is 0.036 , which is slightly higher than district 6, at 0.033 and district 8, at 0.031 . Samen district and district 4 had the same median NDVI of 0.03 . Districts 9 and 5 had the same value, at 0.029 . Districts 10 and 2 had the same value of 0.024 . The median NDVI of district 1 was 0.02 which was slightly higher than district 11, at 0.19 . According to the boxplot, the NDVI range between all districts is not equal. Therefore, the next section provides NDVI distributions which can be used to understand the density and range of green spaces within each district.

4.3. NDVI distribution in all districts of the study area

This section shows NDVI distributions by calculating the cumulative histogram of an image. Based on the NDVI greyscale, the histograms represent changes in grey brightness in four districts of Mashhad. Vegetated land was identified as dark areas while brighter areas represented bare soil and built-up areas. According to this explanation, districts with a higher density of darker areas are considered to be greener. An image's histogram with a skew that is closer to the left has darker pixels (Figure 4). The histogram shows the density and range of green spaces in each district based on NDVI greyscale frequencies. Due to the greater number of darker pixels in districts 1, 8, 9, 11, and 12, the histogram positioned closer to the left exhibited a greater distribution of NDVI. There was a skew to the right in districts 2, 3, 4, 5, 6, 7, and 10 with a low

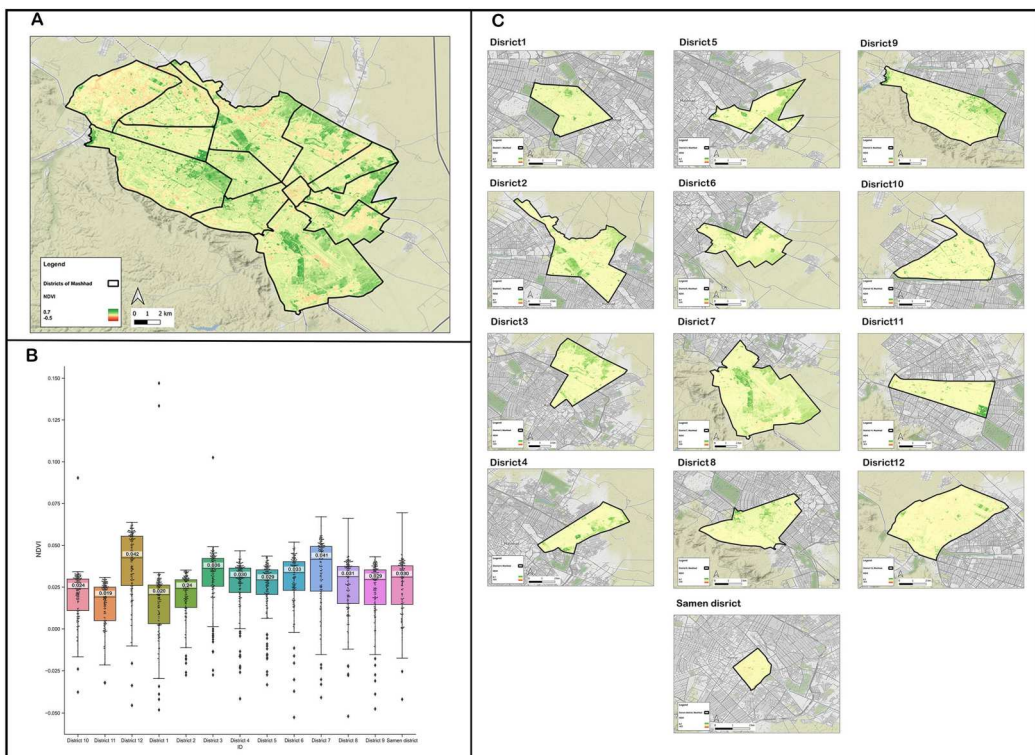


Figure 3. (A) NDVI variation; (B) Comparison median NDVI of all. (C) Comparison NDVI of all districts.

density of green spaces. We, therefore, provide evidence regarding how the distribution of green spaces impacts LST. It is more important to consider the range and density of the NDVI value rather than its median.

4.4. Network analyses

We examined the impact of network measurements on UHI. We explored the relationship between street network measurements and LST using Momepy and OSMnx open-source Python libraries. We visualized street pattern measurements such as straightness and local closeness-centrality. These two indexes describe two opposite types of network pattern. Straightness is an indication that all spaces are more integrated and straight. In contrast, local closeness-centrality indicates that all streets are located near one another, therefore, all the urban features in these types of areas are located closely together. Developing green spaces can mitigate the effects of UHI. However, if you have a dense network of streets, then this effect is minimal. The street pattern type limits the cooling effect of shading from trees.

4.4.1. Street local closeness-centrality variation in all districts of the study area

In the analysis of urban street patterns in Mashhad, the points in each network graph have a different level (purple, dark blue, dark green, light green, and yellow): Yellow points have the highest value, green points have the middle value, and purple and dark blue points have the lowest value. The yellow areas are highly close to their neighbouring features (Figure 5). Green areas represent street patterns that are less closely spaced. Blue and purple areas indicate the lowest level of closeness (Lobsang, Zhen, and Zhang 2019). Based on the density and location of the skew, we can determine the degree of closeness of each district. Skews located more to the right with a higher density have a higher closeness-centrality value. The lowest value for local closeness-centrality was recorded in district 12 and the highest was recorded in district 5. Based on the boxplots, almost the same range was recorded in each district.

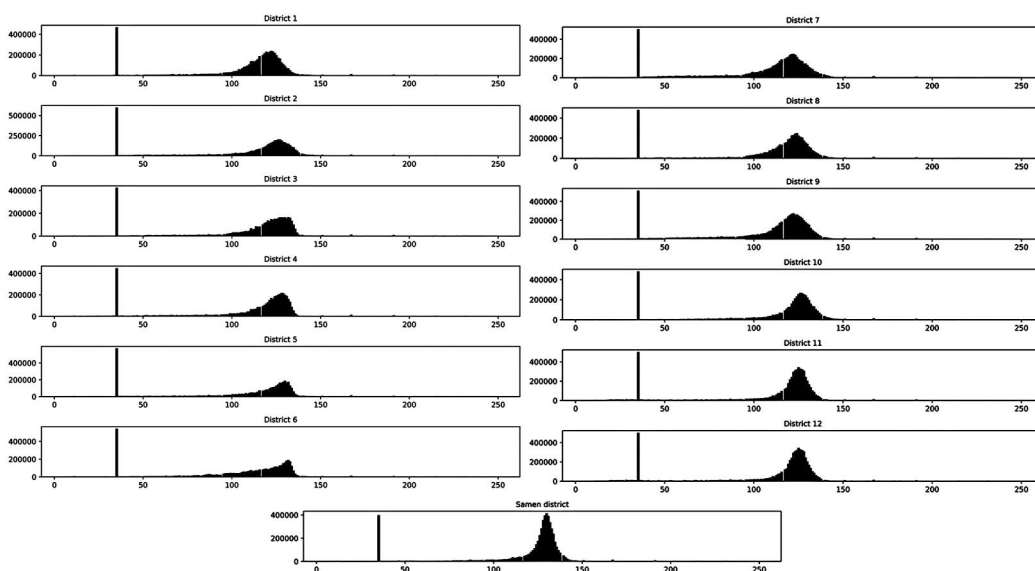


Figure 4. Comparison of NDVI between districts.

4.4.2. Street straightness variation in all districts of the study area

By comparing local closeness-centrality with LST, we provided evidence for higher temperatures in the closer pattern (Figure 6). Based on the bell curve distribution, the low value of straightness was recorded in district 4 and the high value belonged to district 1. Districts with high straightness values had lower temperatures.

4.5. Relationship between LST, NDVI, straightness and local closeness-centrality

According to Figure 7 Pearson's correlation coefficient was -0.9455 , -0.9633 , and $+0.9605$ respectively between LST and NDVI, straightness and local closeness-centrality. The relationship between NDVI and straightness was negatively correlated with LST, whereas the relationship between local closeness-centrality and LST was positively correlated. It follows that UHI has a strong direct relationship with local closeness-centrality, but a strong indirect relationship with straightness and NDVI. Correlation results indicate that street measurements and LST have a stronger relationship than NDVI and LST. Sustainable urban planning and design require a holistic approach to viewing the entire city as a whole in order to reduce surface temperatures within a city. According to this approach, the NDVI degree should not be the only factor that influences surface temperature. It is important to consider other aspects of the urban surface as well.

5. Discussion

Mashhad's dry climate makes expanding green spaces and green roofs costly; thus, street pattern indexes can be considered as sustainable approach for heat control. This study examined the impact of urban street pattern as an urban feature on UHI. Previous studies (Alves, Anjos, and Galvani 2020; Portela et al. 2020; Yang et al. 2019) have focused more on the NDVI degree. Built-up features such as buildings, roads, or other urban structures absorb and re-emit more heat than natural

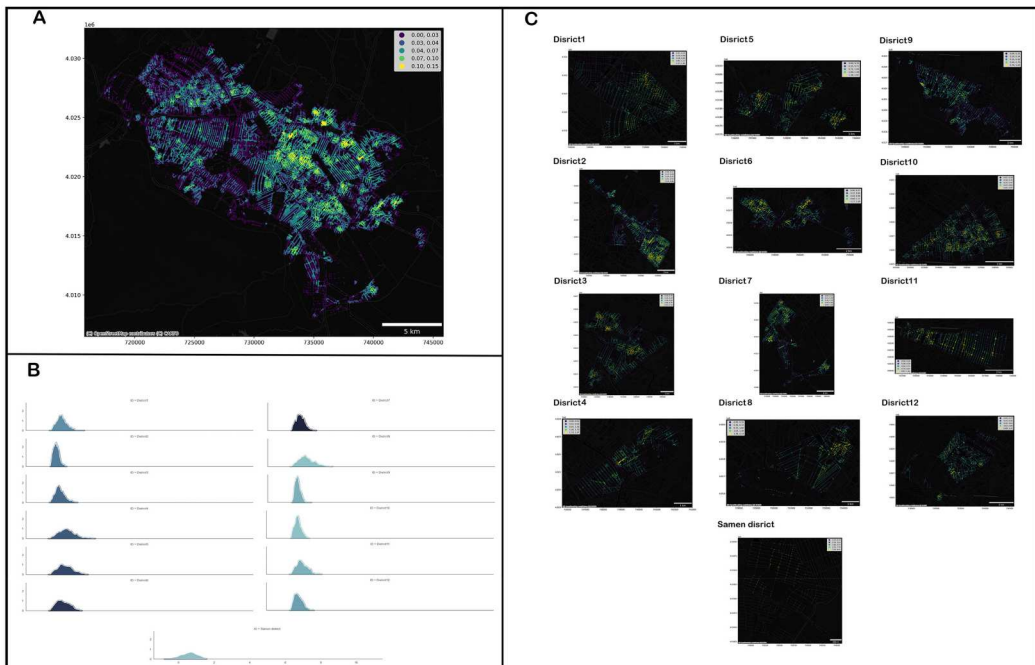


Figure 5. (A) Closeness-centrality variation; (B) Closeness-centrality density of all districts; (C) Closeness-centrality of all districts.

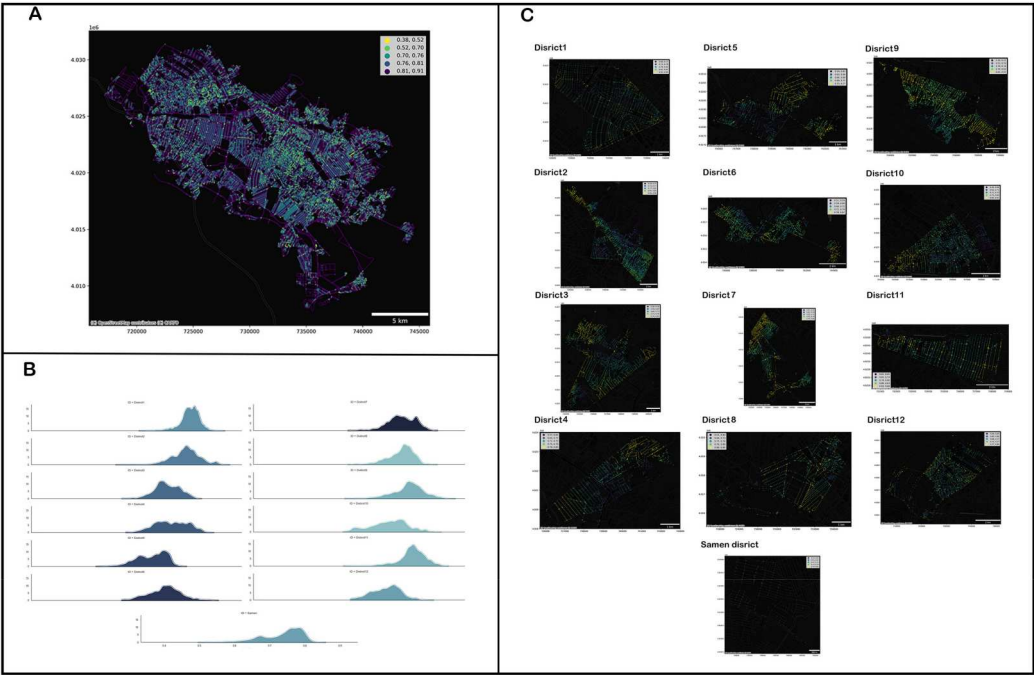


Figure 6. (A) Straightness variation; (B) Straightness density of all districts; (C) Straightness of all districts.

landscapes such as parks or lakes. A built-up area affects UHI similarly to NDVI, since both are surface features. Roads and streets are particularly important as they cover a substantial portion of urban surface. Street patterns determine how other urban elements are positioned and distributed in cities (Erdem, Mert Cubukcu, and Sharifi 2021). As street networks could remain unchanged for many years, they have long-term consequences for urban warming.

To make the comparison, all 12 districts of Mashhad metropolis were selected. Moreover, three indicators of NDVI distribution, local closeness-centrality, and straightness were used to assess the relationship between street pattern indices and LST. A combination of tools including; GEE, also Network Analysis, and Image Processing was used.

According to the findings, the higher straightness of the street pattern, the lower LST, whereas the higher local closeness-centrality of street pattern, the higher the LST. In street pattern that is characterized by high local closeness-centrality and low straightness, urban elements are often close to each other and there is not enough space between buildings. Therefore, satellites observe more build-up reflection in this kind of pattern, which is the result of a high surface temperature. The results indicated that patterns with high straightness and low closeness-centrality had lower

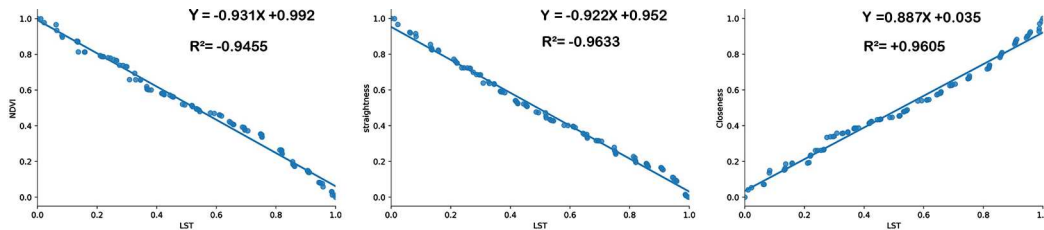


Figure 7. Pearson correlation between LST and NDVI, closeness-centrality, and Straightness.

UHI effect. It can, therefore, be argued that patterns with high levels of straightness and low levels of closeness are more resilient against urban heat stress. Patterns featuring high levels of straightness are also argued to be more resilient against other types of stressors. For instance, it is argued that higher straightness enables better connection between nodes in a street network, thereby contributing to improved emergency response when needed (Sharifi 2019). However, lower levels of closeness centrality are not always desirable for building urban resilience to other stressors. For instance, higher closeness centrality is desirable for better accessibility of emergency services or for enhancing economic vibrancy and resilience (Sharifi 2019). Accordingly, trade-offs may emerge when deciding to promote patterns that facilitate balanced resilience against different stressors. It is essential to develop optimal patterns that minimize such trade-offs. We also found that high NDVI degree and NDVI distribution (a measure of the distribution of green spaces across an area) were associated with lower surface temperatures. Generally, a moderate-grid pattern with a reasonable distribution of green spaces throughout the region reduces surface temperatures sustainably. Indeed, adding greenery to areas with higher closeness centrality could be helpful in mitigating the heat effects.

Erdem, Mert Cubukcu, and Sharifi (2021) and Mohamed et al. (2021) found that higher street network connectivity is associated with lower levels of the UHI effect. Such networks are characterized by a high degree of straightness, and low degrees of local closeness-centrality. We analysed each of the above factors with LST. Erdem, Mert Cubukcu, and Sharifi (2021) found a specific relationship between local closeness-centrality and LST based on a T-test of 0.25. Mohamed et al. (2021) overlaid two LST maps and the connectivity map of the network in order to examine their point. Therefore, they did not test the data to verify the accuracy and reliability of their results. Our study confirms their findings. However, when comparing the results of the proposed method with those of the conventional methods of these previous studies, it should be noted that we calculated each index using coding. A significant Pearson correlation of -0.9455 , -0.9633 , and $+0.9605$ was recorded for LST, with Mean NDVI, straightness, and local closeness-centrality. We also found a moderate grid street pattern reflecting 1.7161°C lower temperatures than pure grid street patterns. A similar conclusion was reached by (Sobstyl et al. 2018). A grid pattern is similar to crystal, with the exact same pattern repeating, but a pattern with a lesser similarity is comparable to glass, which is more durable than crystal (Sobstyl et al. 2018).

What is surprising is that the NDVI distribution is more significant than the NDVI itself. Thus, it is more important to plan for distributing green spaces in an area rather than expanding huge public parks just for the sake of increasing NDVI degree. We compared two distinct districts, one with a higher NDVI degree, but with a lower NDVI distribution (district 6), and the other with a lower NDVI degree, but with a higher NDVI distribution (district 1). However, the second district reflected a lower temperature. This leads us to the importance of establishing for green spaces in cities.

6. Conclusion

This research examines the relationship between urban street network measurements and LST in Mashhad, Iran. The findings suggest that a moderate-grid pattern with a reasonable distribution of green spaces throughout the region can reduce surface temperatures sustainably. The study also confirmed previous findings that urban form and texture can influence the UHI effect (Soltani and Sharifi 2017). The research provided insight into the importance of considering street network measurements in long-term urban planning and design to improve urban resilience, and mitigate the UHI effect in arid regions.

This research has important policy implications for urban planning and design. The study suggests that long-term planning and design that prioritizes a moderate grid street pattern with a reasonable distribution of green spaces throughout the region can help reduce surface temperatures sustainably. The findings of the study highlight the importance of considering street network measurements such

as straightness and local closeness-centrality in urban design to mitigate the UHI effect. Urban designers can use this information to create a street network pattern that has a lower UHI effect by reducing the degree of local closeness-centrality and increasing the degree of straightness. However, making such changes could be challenging and costly in existing urban textures due to lock-in effects. Under such circumstances, Mashhad's future development should be based on designing street patterns that balance closeness-centrality and straightness. Other measures, such as NDVI distribution, should be prioritised for mitigating UHI in existing textures. Such measures should, particularly, be prioritised in parts of the city that feature high levels of closeness centrality and low straightness. For instance, green spaces should be well distributed in all areas of districts with high closeness-centrality. Due to the arid climate of the study area, it is recommended that greening in districts with high closeness-centrality be achieved through planting trees with low water requirements that are well distributed throughout the study area. The study also suggests that urban textures, such as building heights, the depth of building plans, and the layout of urban areas, can play a significant role in enhancing UHI. This information can help policymakers and urban planners optimize urban textures and control key morphological features to enhance UHI. Finally, the study highlights the importance of NDVI distribution in reducing surface temperatures sustainably. Policymakers and urban planners can prioritize green spaces in urban areas and ensure a reasonable distribution of green spaces throughout the region to reduce the UHI effect.

While this study provides valuable insights into the relationship between urban street patterns and UHI in Mashhad, Iran, there are several limitations that suggest opportunities for future research. One of the aspects of UHI is the simulation of streets, buildings, and the arrangement of urban features. Future studies should include simulations with a focus on street patterns. The simulation model can include street patterns with different street orientations and different degrees of closeness, centrality, and straightness. This can be accomplished by adding different levels of NDVI distributions according to each potential street pattern. There is also the possibility of modifying the material and density of buildings in this model, but one noticeable factor is the street pattern indices, which arrange urban features, and by modifying the indices that we evaluated in this study, researchers can create an interesting simulated environment. By using the simulation model described above, urban planners can better understand how street patterns can be designed to be environmentally sustainable. This study had the limitation of not determining the relationship between street pattern indexes and LST in different seasons and at different times of the day. Future studies should be simulated or analysed in different time periods. The study's limited scope only focused on Mashhad, and further research is needed to examine the generalizability of the findings to other cities with different urban and climatic characteristics. The use of remote sensing data from GEE may have limitations in terms of accuracy and resolution, and more reliable data collection methods such as field observations and micro-scale temperature measurements could be explored in future research. Further research could explore alternative methods to validate the findings. Additionally, while the study established correlations between urban street patterns and UHI, more research is needed to establish causality, and other factors contributing to the observed patterns should be explored. Furthermore, larger sample sizes may be necessary to confirm the findings. Finally, the study did not provide information on the characteristics of the sample, such as demographic and socioeconomic factors, which may have an impact on UHI, and further research could explore these factors.

Acknowledgements

The authors would like to thank the editor and three anonymous reviewers for their inputs that helped to significantly improve the quality of the manuscript.

Disclosure statement

No potential conflict of interest was reported by the author(s).

Data availability

The data that support the findings of this study are available on request from the corresponding author.

ORCID

Ali Soltani  <http://orcid.org/0000-0001-8042-410X>

Ayyoob Sharifi  <http://orcid.org/0000-0002-8983-8613>

References

- Abd Elaziz, Mohamed, Neggaz Nabil, Reza Moghdani, Ahmed A Ewees, Erik Cuevas, and Songfeng Lu. 2021. "Multilevel Thresholding Image Segmentation Based on Improved Volleyball Premier League Algorithm Using Whale Optimization Algorithm." *Multimedia Tools and Applications* 80 (8): 12435–12468. <https://doi.org/10.1007/s11042-020-10313-w>.
- Abdollahzadeh, Nastaran, and Nimish Bioria. 2021. "Outdoor Thermal Comfort: Analyzing the Impact of Urban Configurations on the Thermal Performance of Street Canyons in the Humid Subtropical Climate of Sydney." *Frontiers of Architectural Research* 10 (2): 394–409. <https://doi.org/10.1016/j.foar.2020.11.006>.
- Allan, A., A. Soltani, M. H. Abdi, and M. Zarei. 2022. "Driving Forces Behind Land Use and Land Cover Change: A Systematic and Bibliometric Review." *Land* 11 (8): 1222. <https://doi.org/10.3390/land11081222>.
- Altaweel, Mark, Jack Hanson, and Andrea Squitieri. 2021. "The Structure, Centrality, and Scale of Urban Street Networks: Cases from Pre-Industrial Afro-Eurasia." *PLoS One* 16 (11): e0259680–e0259680. <https://doi.org/10.1371/journal.pone.0259680>.
- Alves, Elis, Max Anjos, and Emerson Galvani. 2020. "Surface Urban Heat Island in Middle City: Spatial and Temporal Characteristics." *Urban Science* 4 (4): 54. <https://doi.org/10.3390/urbansci4040054>.
- Amanzadeh, Naser, Toshihide H Arimura, Mohammad Vesal, and Seyed Farshad Fatemi Ardestami. 2021. "The Distributional Effects of Climate Change: Evidence from Iran." *SSRN Electronic Journal*, <https://doi.org/10.2139/ssrn.3795067>.
- Azhdari, Abolghasem, Ali Soltani, and Mehdi Alidadi. 2018. "Urban Morphology and Landscape Structure Effect on Land Surface Temperature: Evidence from Shiraz, a Semi-Arid City." *Sustainable Cities and Society* 41: 853–864. <https://doi.org/10.1016/j.scs.2018.06.034>.
- Azizi, P., A. Soltani, F. Bagheri, S. Sharifi, and M. Mikaeili. 2022. "An Integrated Modelling Approach to Urban Growth and Land Use/Cover Change." *Land* 11 (10): 1715. <https://doi.org/10.3390/land11101715>.
- Bagheri, Bagher, and Ali Soltani. 2023. "The Spatio-Temporal Dynamics of Urban Growth and Population in Metropolitan Regions of Iran." *Habitat International* 136: 102797. <https://doi.org/10.1016/j.habitatint.2023.102797>.
- Barthelemy, M. A. R. C. 2022. *Spatial Networks: A Complete Introduction*. Cham: Springer.
- Boeing, Geoff. 2017. "OSMnx: New Methods for Acquiring, Constructing, Analyzing, and Visualizing Complex Street Networks." *Computers, Environment and Urban Systems* 65: 126–139. <https://doi.org/10.1016/j.compenvurbsys.2017.05.004>.
- Erdem, Umut, K. Mert Cubukcu, and Ayyoob Sharifi. 2021. "An Analysis of Urban Form Factors Driving Urban Heat Island: The Case of Izmir." *Environment, Development and Sustainability* 23 (5): 7835–7859. <https://doi.org/10.1007/s10668-020-00950-4>.
- Fleischmann, Martin, Alessandra Feliciotti, and William Kerr. 2022. "Evolution of Urban Patterns: Urban Morphology as an Open Reproducible Data Science." *Geographical Analysis* 54 (3): 536–558. <https://doi.org/10.1111/gean.12302>.
- Ghanbari, R., M. Heidarimozaffar, A. Soltani, and H. Arefi. 2023. "Land Surface Temperature Analysis in Densely Populated Zones from the Perspective of Spectral Indices and Urban Morphology." *International Journal of Environmental Science and Technology* 20. <https://doi.org/10.1007/s13762-022-04725-4>.
- Grubb, Jacob, Derek Lopez, Bhuvaneshwar Mohan, and John Matta. 2021. "Network Centrality for the Identification of Biomarkers in Respondent-Driven Sampling Datasets." *PLoS One* 16 (8): e0256601–e0256601. <https://doi.org/10.1371/journal.pone.0256601>.
- Han, Dongrui, Hongmin An, Fei Wang, Xinliang Xu, Zhi Qiao, Meng Wang, Xueyan Sui, et al. 2022. "Understanding Seasonal Contributions of Urban Morphology to Thermal Environment Based on Boosted Regression Tree Approach." *Building and Environment* 226: 109770. <https://doi.org/10.1016/j.buildenv.2022.109770>.
- Hou, Jiajie, Yupeng Wang, Dian Zhou, and Zhe Gao. 2022. "Environmental Effects from Pocket Park Design According to District Planning Patterns – Cases from Xi'an, China." *Atmosphere* 13 (2): 300. <https://doi.org/10.3390/atmos13020300>.

- Howard, Luke. 1818. *The Climate of London: Deduced from Meteorological Observations*. Volume 2. Vol. 1. W. Phillips, George Yard, Lombard Street, sold also by J. and A. Arch ...
- Irons, James R, John L Dwyer, and Julia A Barsi. 2012. "The Next Landsat Satellite: The Landsat Data Continuity Mission." *Remote Sensing of Environment* 122: 11–21. <https://doi.org/10.1016/j.rse.2011.08.026>.
- Kim, Se Woong, and Robert D Brown. 2021. "Urban Heat Island (UHI) Variations Within a City Boundary: A Systematic Literature Review." *Renewable and Sustainable Energy Reviews* 148: 111256. <https://doi.org/10.1016/j.rser.2021.111256>.
- Kleerekoper, Laura, Marjolein Van Esch, and Tadeo Baldiri Salcedo. 2018. "How to Make a City Climate-Proof: Addressing the Urban Heat Island Effect." *Planning for Climate Change: A Reader in Green Infrastructure and Sustainable Design for Resilient Cities* 64: 250–262. <https://doi.org/10.1016/j.resconrec.2011.06.004>.
- Kong, Jing, Yongling Zhao, Jan Carmeliet, and Chengwang Lei. 2021. "Urban Heat Island and Its Interaction with Heatwaves: A Review of Studies on Mesoscale." *Sustainability (Switzerland)* 13 (19): 10923. <https://doi.org/10.3390/su131910923>.
- Lee, Kirim, Jihoon Seong, Youkyung Han, and Won Hee Lee. 2020. "Evaluation of Applicability of Various Color Space Techniques of UAV Images for Evaluating Cool Roof Performance." *Energies* 13 (6): 4213. <https://doi.org/10.3390/en13164213>.
- Lin, Jingyi, and Yifang Ban. 2017. "Comparative Analysis on Topological Structures of Urban Street Networks." *ISPRS International Journal of Geo-Information* 6 (10): 295. <https://doi.org/10.3390/ijgi6100295>.
- Lobsang, Tashi, Feng Zhen, and Shanqi Zhang. 2019. "Can Urban Street Network Characteristics Indicate Economic Development Level? Evidence from Chinese Cities." *ISPRS International Journal of Geo-Information* 9 (1): 3. <https://doi.org/10.3390/ijgi9010003>.
- Marshall, Stephen. 2004. *Streets and Patterns*. London: Routledge. <https://doi.org/10.4324/9780203589397>.
- Masoumi, Houshmand E. 2015. "Transformation of Urban Form and the Effects on Travel Behavior in Iran." *Annals of Statistics* 33 (1): 1–33. http://www.tu-berlin.de/ztg/menue/publikationen/discussion_papers/.
- Mesgaran, Mohsen B, and Pooya Azadi. 2018. "A National Adaptation Plan for Water Scarcity in Iran." In *Working Paper 6, Stanford Iran 2040 Project, Stanford University, August 2018*, 37. https://www.researchgate.net/publication/327070709_A_National_Adaptation_Plan_for_Water_Scarcity_in_Iran.
- Moghadam, A. S., A. Soltani, and B. Parolin. 2018a. "Transforming and changing urban centres: The experience of Sydney from 1981 to 2006." *Letters in Spatial and Resource Sciences* 11 (1): 37–53. <https://doi.org/10.1007/s12076-017-0197-7>.
- Moghadam, A. S., A. Soltani, B. Parolin, and M. Alidadi. 2018b. "Analysing the space-time dynamics of urban structure change using employment density and distribution data." *Cities* 81: 203–213. <https://doi.org/10.1016/j.cities.2018.04.009>.
- Mohamed, Mady, Abdullah Othman, Abotalib Z Abotalib, and Abdulrahman Majrashi. 2021. "Urban Heat Island Effects on Megacities in Desert Environments Using Spatial Network Analysis and Remote Sensing Data: A Case Study from Western Saudi Arabia." *Remote Sensing* 13 (10): 1941. <https://doi.org/10.3390/rs13101941>.
- Nagy, Attila, Andrea Szabó, Odunayo David Adeniyi, and János Tamás. 2021. "Wheat Yield Forecasting for the Tisza River Catchment Using Landsat 8 Nvdi and Savi Time Series and Reported Crop Statistics." *Agronomys Note: MDPI stays neutral with regard to jurisdictional claims in ...* <https://doi.org/10.3390/agronomy11040652>.
- Naserikia, Marzie, Elyas Asadi Shamsabadi, Mojtaba Rafieian, and Walter Leal Filho. 2019. "The Urban Heat Island in an Urban Context: A Case Study of Mashhad, Iran." *International Journal of Environmental Research and Public Health* 16 (3): 313. <https://doi.org/10.3390/ijerph16030313>.
- Nasseh, S., N. Hafezi Moghaddas, M. Ghafoori, O. Asghari, and J. Bolouri Bazaz. 2016. "Spatial Variability Analysis of Subsurface Soil in the City of Mashhad, Northern- East Iran." *International Journal of Mining and Geo-Engineering* 50 (2): 219–229. <https://doi.org/10.22059/ijmge.2016.59832>.
- Omer, Itzhak, and Orna Zafrir-Reuven. 2015. "The Development of Street Patterns in Israeli Cities." *Journal of Urban and Regional Analysis* 7 (2): 113–127. <https://doi.org/10.37043/jura.2015.7.2.1>.
- Porta, Sergio, Paolo Crucitti, and Vito Latora. 2006. "The Network Analysis of Urban Streets: A Primal Approach." *Environment and Planning B: Planning and Design* 33 (5): 705–725. <https://doi.org/10.1068/b32045>.
- Portela, Carina Inácio, Klécia Gili Massi, Thanan Rodrigues, and Enner Alcântara. 2020. "Impact of Urban and Industrial Features on Land Surface Temperature: Evidences from Satellite Thermal Indices." *Sustainable Cities and Society* 56: 102100. <https://doi.org/10.1016/j.scs.2020.102100>.
- Qasemipour, Ehsan, Farhad Tarahomi, Markus Pahlow, Seyed Saeed Malek Sadati, and Ali Abbasi. 2020. "Assessment of Virtual Water Flows in Iran Using a Multi-Regional Input-Output Analysis." *Sustainability (Switzerland)* 12 (18): 7424. <https://doi.org/10.3390/su12187424>.
- Qiao, Zhi, Yingshuang Lu, Tong He, Feng Wu, Xinliang Xu, Luo Liu, Fang Wang, Zongyao Sun, and Dongrui Han. 2023. "Spatial Expansion Paths of Urban Heat Islands in Chinese Cities: Analysis from a Dynamic Topological Perspective for the Improvement of Climate Resilience." *Resources, Conservation and Recycling* 188: 106680. <https://doi.org/10.1016/j.resconrec.2022.106680>.
- Ramyar, Reza. 2019. "Social-Ecological Mapping of Urban Landscapes: Challenges and Perspectives on Ecosystem Services in Mashhad, Iran." *Habitat International* 92: 102043. <https://doi.org/10.1016/j.habitatint.2019.102043>.

- Ren, Jiayi, Jun Yang, Yuqing Zhang, Xiangming Xiao, Jianhong Cecilia Xia, Xueming Li, and Shaohua Wang. 2022. "Exploring Thermal Comfort of Urban Buildings Based on Local Climate Zones." *Journal of Cleaner Production* 340: 130744. <https://doi.org/10.1016/j.jclepro.2022.130744>.
- Rosenzweig, C., S. Gaffin, and L. Parshall. 2006. *Green Roofs in the New York Metropolitan Region: Research Report*. New York: Columbia University Center for Climate Systems Research and NASA Goddard Institute for Space Studies.
- Sadeqi, Amin, Hossein Tabari, and Yagob Dinpashoh. 2022. "Spatio-Temporal Analysis of Heating and Cooling Degree-Days Over Iran." *Stochastic Environmental Research and Risk Assessment* 36 (3): 869–891. <https://doi.org/10.1007/s00477-021-02064-3>.
- Sharifi, Ayyoob. 2019. "Resilient Urban Forms: A Review of Literature on Streets and Street Networks." *Building and Environment* 147: 171–187. <https://doi.org/10.1016/j.buildenv.2018.09.040>.
- Sharifi, Ehsan, and Ali Soltani. 2017. *Patterns of Urban Heat Island Effect in Adelaide: A Mobile Traverse Experiment*. Canadian Center of Science and Education.
- Sobstyl, J. M., T. Emig, M. J. Abdolhosseini Qomi, R. J.-M. Pellenq, and F.-J. Ulm. 2017. "Role of Structural Morphology in Urban Heat Islands at Night Time." *APS March Meeting Abstracts* 2017: M1–298. <https://doi.org/10.1103/PhysRevLett.120.108701>.
- Sobstyl, J. M., T. Emig, M. J. Abdolhosseini Qomi, F. J. Ulm, and R. J. M. Pellenq. 2018. "Role of City Texture in Urban Heat Islands at Nighttime." *Physical Review Letters* 120 (10): 108701. <https://doi.org/10.1103/PhysRevLett.120.108701>.
- Solomon, Susan, Dahe Qin, Martin Manning, Kristen Averyt, and Melinda Marquis. 2007. *Climate Change 2007-the Physical Science Basis: Working Group I Contribution to the Fourth Assessment Report of the IPCC. Vol. 4*. Cambridge University Press.
- Soltani, A., and E. Sharifi. 2017. "Daily Variation of Urban Heat Island Effect and its Correlations to Urban Greenery: A Case Study of Adelaide." *Frontiers of Architectural Research* 6 (4): 529–538. <https://doi.org/10.1016/j.foar.2017.08.001>.
- Song, Peihao, Gunwoo Kim, Audrey Mayer, Ruizhen He, and Guohang Tian. 2020. "Assessing the Ecosystem Services of Various Types of Urban Green Spaces Based on I-Tree Eco." *Sustainability (Switzerland)* 12 (4): 1630. <https://doi.org/10.3390/su12041630>.
- Tan, Kanghao, Yinghong Qin, and Junsong Wang. 2022. "Evaluation of the Properties and Carbon Sequestration Potential of Biochar-Modified Pervious Concrete." *Construction and Building Materials* 314: 125648. <https://doi.org/10.1016/j.conbuildmat.2021.125648>.
- Tan, Kanghao, and Junsong Wang. 2023. "Substrate Modified with Biochar Improves the Hydrothermal Properties of Green Roofs." *Environmental Research* 216: 114405. <https://doi.org/10.1016/j.envres.2022.114405>.
- Voogt, James A. 2004. "Urban Heat Islands: Hotter Cities."
- Wu, Wei, Hongyan Ren, Ming Yu, and Zhen Wang. 2018. "Distinct Influences of Urban Villages on Urban Heat Islands: A Case Study in the Pearl River Delta, China." *International Journal of Environmental Research and Public Health* 15 (8): 1666. <https://doi.org/10.3390/ijerph15081666>.
- Yang, Yujie, Shijie Wang, Xiaoyong Bai, Qiu Tan, Qin Li, Luhua Wu, Shiqi Tian, Zeyin Hu, Chaojun Li, and Yuanhong Deng. 2019. "Factors Affecting Long-Term Trends in Global NDVI." *Forests* 10 (5): 372. <https://doi.org/10.3390/f10050372>.
- Yang, Jun, Jiaxing Xin, Yuqing Zhang, Xiangming Xiao, and Jianhong Cecilia Xia. 2022. "Contributions of Sea–Land Breeze and Local Climate Zones to Daytime and Nighttime Heat Island Intensity." *Npj Urban Sustainability* 2 (1): 12. <https://doi.org/10.1038/s42949-022-00055-z>.
- Zendehbad, Mohammad, P. Cepuder, Willibald Loiskandl, and Christine Stumpp. 2019. "Source Identification of Nitrate Contamination in the Urban Aquifer of Mashhad, Iran." *Journal of Hydrology: Regional Studies* 25: 100618. <https://doi.org/10.1016/j.ejrh.2019.100618>.